Observations of the 2-Day Wave in NMC Stratospheric Analyses

WILLIAM J. RANDEL

National Center for Atmospheric Research, Boulder, Colorado*

(Manuscript received 9 February 1993, in final form 7 July 1993)

ABSTRACT

Observational characteristics of the 2-day wave, a westward-propagating zonal wave 3 oscillation in the summer subtropical upper stratosphere and mesosphere, are studied based on five years of National Meteorological Center (NMC) operational stratospheric analyses. These data show episodic occurrence of the 2-day wave in the upper stratosphere in January (centered near 20°S) and July–August (centered near 20°N). These episodes are strongly correlated with observed reversals of the zonal mean potential vorticity gradient near the core of the summer easterly jet, consistent with previous suggestions that the 2-day wave is generated by an in situ instability of this jet. On the other hand, the horizontal and vertical structure of the waves is very similar to that calculated by Salby for a global normal-mode Rossby wave. The combination of normal-mode structure and instability signature suggests that the 2-day wave is a near-resonant mode forced by dynamical instability.

1. Introduction

The 2-day wave is a westward-propagating zonal wave 3 oscillation observed in the upper stratosphere and mesosphere of the subtropics during summer. It has been identified in radar measurements of mesospheric winds over 80–100 km (Craig et al. 1980; Salby and Roper 1980; Craig and Elford 1981, and references therein), rocketsonde wind observations near the stratopause (Coy 1979), and satellite temperature measurements in the upper stratosphere and mesosphere (Rodgers and Prata 1981; Burks and Leovy 1986; Lait and Stanford 1988). Plumb (1983) gives a concise review of the observed characteristics of the 2-day wave. Briefly, the latitude structure shows a maximum near 20° in the summer hemisphere, with in-phase horizontal structure over approximately 0°–50° latitude. There is also suggestion of a weak out-of-phase wave amplitude maximum in the opposite (winter) hemisphere (Tsuda et al. 1988). The 2-day wave amplitude is stronger during the Southern Hemisphere (SH) summer by about a factor of 2 over the Northern Hemisphere (NH) summer. The mode is clearly identified by its sharp frequency peak: the period is near 48–49 h in the SH and near 51–52 h in the NH. Global satellite measurements (referenced above) have unambiguously shown a traveling zonal wave 3–4 structure. One of the most interesting features of the 2-day wave is that it is observed in low to middle latitudes of both hemispheres, with greatly enhanced amplitudes, for a period of several weeks following summer solstice.

Observations covering many years show that the 2-day wave is sharply peaked in wavenumber and frequency, suggesting that it is associated with a normal or resonant mode of the atmosphere. Salby (1981a,b) has calculated the structure of such modes using realistic background wind structures and finds that one such mode is indeed a westward-propagating zonal wave 3 with period near 2 days. The background winds modify the mode so that it reaches large amplitudes only in the summer mesospheric easterlies; this is one explanation for the observed seasonal behavior. The calculated temperature structure for this mode exhibits a peak in the summer subtropics, with a weak out-of-phase maximum in the winter hemisphere. The corresponding perturbation wind fields show largest amplitude for the meridional component, with a maximum in the summer subtropics and a broad in-phase structure spanning low-middle latitudes of both hemispheres [see Fig. 8, Salby (1981b)].

A second mechanism to explain the 2-day wave is that it is forced due to baroclinic instability of the summer easterly jet. Plumb (1983) used a one-dimensional analysis to show that appreciable growth rates can occur in this region given realistic wind shear values. Growth rates in his calculations peaked for zonal wavelengths of order 9000 km (zonal waves 3–4 in the subtropics), with periods near 2 days; this latter value is determined mainly by the advective speed of the background zonal winds (maximum near -70 m s^{-1}). Pfister (1985) extended these calculations to two dimen-

* The National Center for Atmospheric Research is sponsored by the National Science Foundation.

Corresponding author address: Dr. William J. Randel, National Center for Atmospheric Research, P.O. Box 3000, Boulder, CO 80307-3000.

sions, again finding peaks in the unstable wave-growth spectrum at zonal wavenumbers 2–4, with periods of 1.4–3 days. However, Pfister's calculations showed maximum perturbation geopotential height amplitudes over latitudes 40°–60°, contrary to the observed maximum near 20°. Because of the near match in wavenumber and frequency between the resonant normal mode and the unstable mode, a possible explanation of the observed space and time structure of the 2-day wave is that it is some combination of the normal and unstable modes; that is, it is a near-resonant mode excited by baroclinic instability.

In this paper, we show evidence of the 2-day wave in daily operational stratospheric analyses produced at the National Meteorological Center (NMC). Zonal wavenumber–frequency spectra of traveling temperature waves in the upper stratosphere show clear maxima for zonal waves 3–4 with periods of 2–2.5 days in the summer subtropics of both hemispheres. [Because of the once daily sampling, the highest frequency resolved with these data is $(2\ \text{days})^{-1}$.] By reconstructing the wave variance in this frequency band over a time period of five years, we show clear evidence for the episodic appearance of the 2-day wave in January at 20°S and in July–August at 20°N. The meridional and vertical structure of the waves during these episodes is calculated from these data and is found to be in reasonable agreement with the normal-mode calculations of Salby (1981a). Furthermore, these data allow calculation of the background zonal winds and potential vorticity (PV) gradients in conjunction with the wave variance time series. The most important result here is that most of the large amplitude wave events are clearly associated with periods of near-zero or negative PV gradients; these observations strongly argue that the 2-day wave is forced by instability of the summer easterly jet. These observations corroborate the analyses of Burks and Leovy (1986), who also postulate an instability mechanism, based on spatial coincidence between the 2-day wave and regions of negative PV gradient. The combination of 1) normal-mode wave structure and 2) strong association between wave growth and negative PV gradients suggests that the 2-day wave is indeed a near-resonant mode forced by an internal dynamical instability.

2. Data and analyses

The data analyzed here are operational daily temperature and geopotential height grids produced by NMC, covering the time period October 1983–September 1988. Description of the stratospheric operational analyses may be found in Gelman et al. (1986) and references therein. For the time period considered here, the vertical temperature profiles were derived from satellite-measured radiances via linear regression against radiosonde and rocketsonde data. [Following 20 September 1988, the analysis changed to a physical retrieval system (M. Gelman 1992, personal communication), and interestingly, the intensity of the 2-day wave in these data is much weaker in the years following this change in data processing.] The temperature and geopotential height data are synoptically gridded via a successive correction (Cressman) objective analysis, incorporating all data within plus or minus 6 h of 1200 UTC. Note that no a priori horizontal structure is built into the grids by this analysis scheme. The 12-hour binning of the data will reduce the amplitude of the fast-traveling waves analyzed here: averaging of a harmonic wave over one-quarter of its period suggests a reduction in amplitude near 10%. The objective analyses are produced separately for each hemisphere, and data on pressure levels 50, 30, 10, 5, 2, and 1 mb are analyzed here.

Space–time cross-spectral analyses are calculated following the standard formulas presented in Hayashi (1971). Time spectral analyses are performed on 60-day time series centered on January and July, averaged over the three years (out of five) when the 2-day wave is strongest (January 1985, 1986, and 1987, and July 1985, 1986, and 1988; see Figs. 2–4 below). Power spectra are smoothed with a (normalized) 1–4–6–4–1 convolution in frequency. The 2-day wave lies near the Nyquist limit for these daily data, and significant aliasing can and does occur. Aliasing in space–time cross-spectral analysis appears as a folding about the Nyquist frequency [$(2\ \text{days})^{-1}$ here] of unresolved westward-propagating variance into eastward power; this is clearly shown below. The band-integrated spectral power and coherence/phase calculations are thus made here by summing both westward- and eastward-propagating variance in the period range 2.0–2.5 days [although the prior analyses of Rodgers and Prata (1981), Burks and Leovy (1986), and Lait and Stanford (1988) clearly show that the 2-day wave propagates westward]. Degrees of freedom (df) for the coherence squared are estimated at 24: (2 df per independent Fourier harmonic in the frequency band) × 4 (a conservative estimate of the number of independent harmonics for eastward plus westward periods of 2.0–2.5 days) × 3 (number of years in the ensemble average). The resulting 95% confidence level for the coherence squared is then near 0.24.

3. Results

The 2-day wave in the NMC data is more pronounced in temperature than in geopotential height data; hence, wave activity is quantified here in terms of transient temperature variability. Figure 1 shows zonal wavenumber–frequency spectra for traveling temperature waves at 1 mb during January (at 20°S) and during July (at 20°N). Both spectra show clear maxima for westward-propagating zonal wave 3 with periods close to 2 days; the spectra for July show the important contribution for zonal wave 4, also. Both spectra also

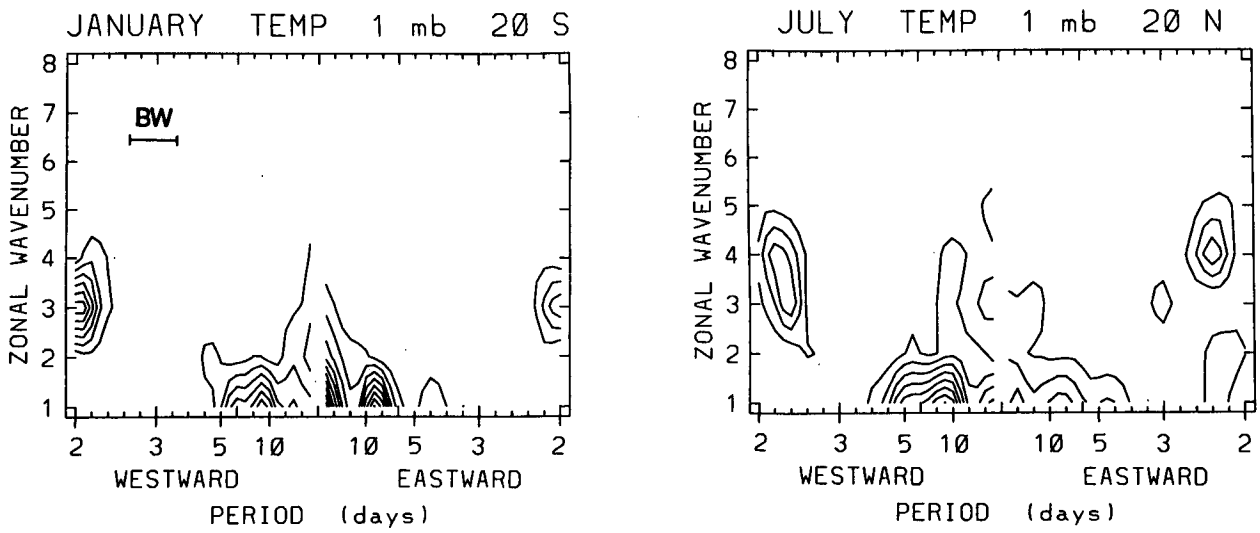

FIG. 1. Zonal wavenumber–frequency power spectra for traveling temperature waves at 1 mb, 20°S in January (left), and 20°N in July (right). The approximate spectral bandwidth (BW) is shown at left. Contours are .008, .012, .016, . . . $K^2 \cdot \Delta\omega^{-1}$.

show variance maxima for eastward-traveling waves at high frequencies, and as discussed above, this likely results from aliasing of westward-propagating waves with periods slightly shorter than 2.0 days. For example, the eastward wave 4 maximum centered near 2.3-day period in July in Fig. 1 is likely an aliased westward-propagating wave with period near 1.8 days, similar to that identified by Burks and Leovy (1986) and Lait and Stanford (1988). As discussed above, we isolate the 2-day wave structure and temporal variation by summing contributions for both westward- and eastward-propagating zonal waves 3–4 with periods of 2.0–2.5 days; hereafter, we refer to this summed contribution as simply the 2-day wave.

Figure 2 shows time variation of the 2-day wave temperature variance at 1 mb and 20°S throughout the five-year data record. This calculation is made by Fourier analysis of the zonal wave coefficient time series, followed by resynthesis for periods of 2.0–2.5 days, and then by calculation of the variance. Also shown in Fig. 2 are the zonal mean zonal wind $\bar{u}$ at this location calculated from the NMC geopotential height data, as well as the quasigeostrophic potential vorticity gradient $\bar{q}_y$:

$$\bar{q}_y = \frac{2\Omega}{a}\cos\phi - \frac{1}{a^2}\frac{\partial}{\partial\phi}\left[\frac{1}{\cos\phi}\frac{\partial}{\partial\phi}(\bar{u}\cos\phi)\right] - (2\Omega\sin\phi)^2 e^{z/H}\frac{\partial}{\partial z}\left[e^{-z/H}\frac{1}{N^2}\frac{\partial\bar{u}}{\partial z}\right],$$

where notation is standard, following Andrews et al. (1987). Variations in $\bar{q}_y$ are examined as a measure of the stability of the zonal mean flow: regions of $\bar{q}_y < 0$ indicate the possibility of internal instability (Andrews et al. 1987, section 5.5.1). The temperature–wave variance time series in Fig. 2 shows maxima during each January, with relatively weak variance during the rest of the year. These 2-day wave variance maxima coincide each year with the most intense summer easterlies (in excess of 50 m s^{-1} each year). Furthermore, the strong wave events during January 1985, 1986, and 1987 are seen to coincide with time periods when $\bar{q}_y < 0$ at this location, consistent with the idea that the wave is associated with an instability of the easterly jet. It is important to note that the instability relationship between negative $\bar{q}_y$ and wave amplitude growth is not necessarily local; that is, $\bar{q}_y$ may become negative in an isolated region, leading to wave growth over a larger (and possibly distant) region. Clear examples of this can be seen in the calculations of Plumb (1983) and Pfister (1985). For most of the large amplitude wave events here, we observe $\bar{q}_y < 0$ to coincide with temperature variance maxima; for cases where the waves grow and $\bar{q}_y$ exhibits a minimum but is not negative (such as January 1984 and 1988 in Fig. 2), we postulate that the source of the instability is above 1 mb (the upper level of the NMC data).

Figure 3 shows a higher time resolution view of variations at 1 mb during the wave event of January 1986. The 2-day wave temperature variance shows three distinct pulses in January, centered over latitudes 0°–30°S, each lasting for approximately one week. The first wave pulse follows a period of approximately two weeks during which $\bar{q}_y < 0$ (noted by the shading in Fig. 3), and the wave growth is seen to be coincident with both deceleration of the jet core near 20°S and removal of the unstable signature. A similar observation of zonal wind deceleration accompanying a wave pulse was shown by Plumb et al. (1987). A small region of $\bar{q}_y < 0$ is also observed in Fig. 3, near the jet core prior to the second wave pulse. The observations of 1) wave growth following the presence of unstable

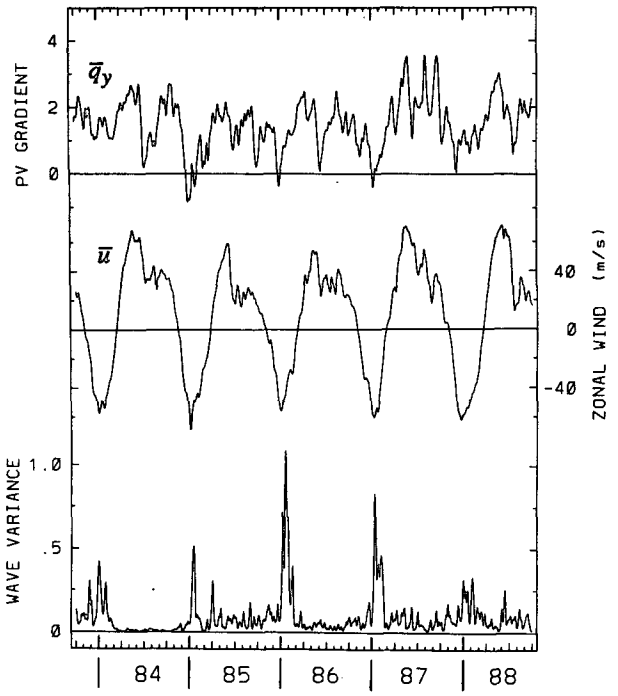

FIG. 2. Lower curve shows time series of 2-day wave temperature variance at 1 mb, 20°S, synthesized from zonal waves 3–4 with periods 2–2.5 days, as discussed in text. The time series covers October 1983–September 1988. Note the episodic variance maxima observed during January of each year. The middle and upper curves show the zonal mean zonal wind $\bar{u}$ (m s^{-1}) and meridional PV gradient $\bar{q}_y$(10^{-11} m^{-1} s^{-1}), both at 1 mb, 20°S. Note the coincidence between wave events, strongest easterly winds, and near-zero values of $\bar{q}_y$.

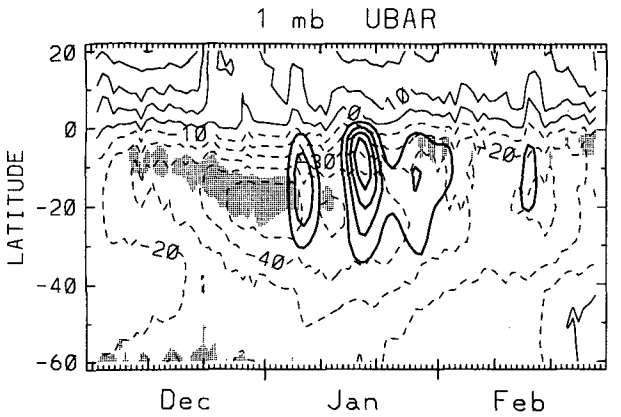

FIG. 3. Latitude–time section of variations at 1 mb during December 1985–February 1986. Thick lines are isopleths of 2-day wave temperature variance, with contours of 0.5 K^2. Thin lines show contours of zonal mean zonal wind $\bar{u}$, and shading denotes locations where the meridional PV gradient is negative ($\bar{q}_y < 0$).

mean flows and 2) wave growth coincident with mean flow deceleration and removal of the unstable signature are strong circumstantial evidence that the 2-day wave results from an instability of the summer easterly jet.

Figure 4 shows time series at 1 mb, 20°N of 2-day wave temperature variance, $\bar{u}$ and $\bar{q}_y$. Here maxima in 2-day wave variance are observed during July–August of 1984, 1985, 1986, and 1988, again nearly coincident with the strongest easterlies (of order 20–30 m s^{-1}, somewhat weaker than the January maxima in Fig. 2). No 2-day wave event is seen in July–August 1987. The $\bar{q}_y$ time series shows near-zero values during July–August 1986 and 1988 (the two strongest wave events), consistent with an instability source mechanism. The wave events during 1984 and 1985 are not coincident with $\bar{q}_y < 0$ at 1 mb, although it is possible that the unstable region lies somewhat above the 1-mb level.

The wave variance time series in Fig. 4 also shows an isolated spike in December 1987, timed differently from the other regular maxima in Figs. 2 and 4. The fast variability for waves 3–4 at this time is associated with a broad spectrum of wave transience in the NH associated with a stratospheric warming event (note the coincident strong $\bar{u}$ deceleration seen in Fig. 4). This event is fundamentally distinct from the other 2-day wave maxima identified here and is not discussed further.

Figure 5 shows the time series of the 2-day wave temperature variance at 1 mb, 20°N and S, with each year's data overlaid to illustrate more clearly the seasonal variation. At both latitudes, the variance maxima occur over approximately two-month intervals: Janu-

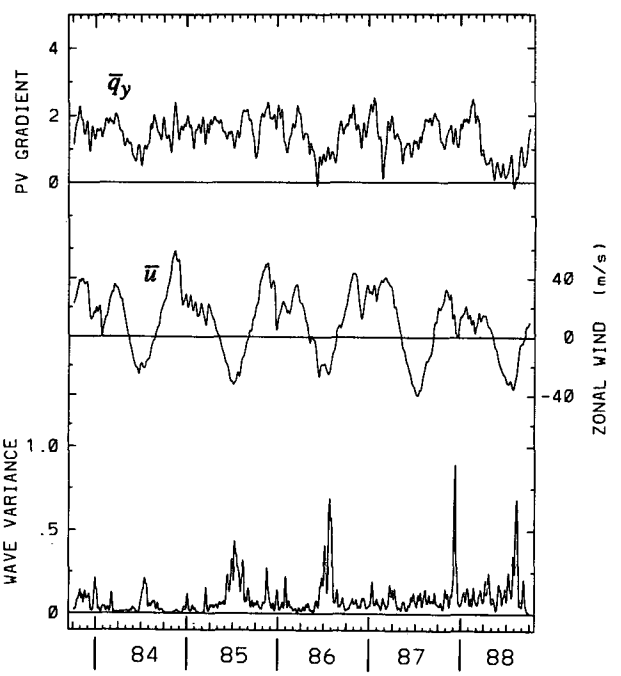

FIG. 4. As in Fig. 2, but for variations at 1 mb, 20°N. Note the 2-day wave events in July–August 1984, 1985, 1986, and 1988. As discussed in the text, the wave variance peak in December 1987 is related to a NH stratospheric warming event, fundamentally distinct from the other maxima.

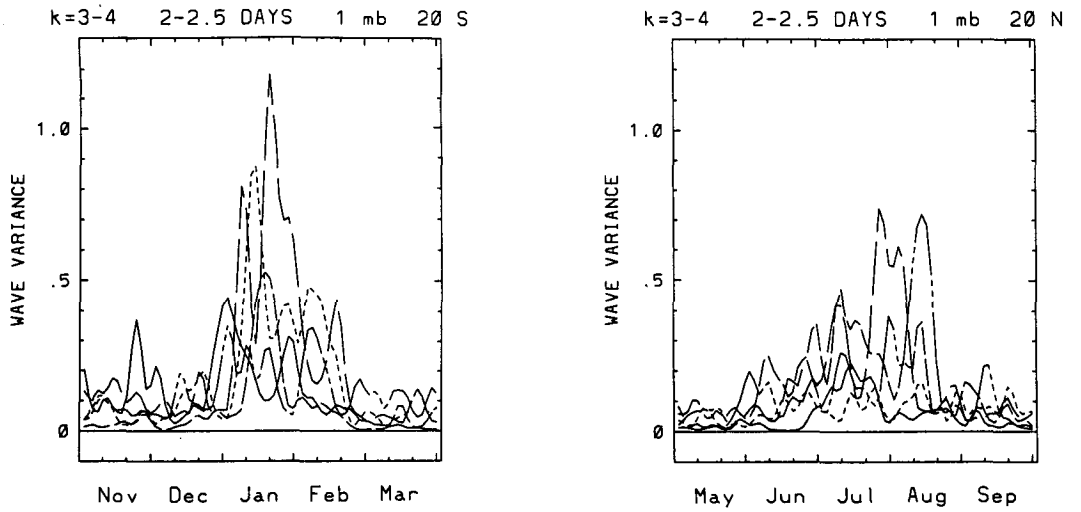

FIG. 5. Time series of 2-day wave temperature variance for each of the five years of data, overlaid on top of each other to demonstrate the observed seasonality and repeatability. Data are shown for 1 mb, 20°S (left), and 20°N (right).

ary–February at 20°S and July–August at 20°N. The limited sample of five years suggests that the 2-day wave is somewhat stronger and more repeatable at 20°S as compared to 20°N.

The temperature variance structure of the 2-day wave in the meridional plane is shown for January in Fig. 6 and July in Fig. 7, along with the corresponding zonal mean zonal winds. As discussed in section 2, these are calculated for each season from the three individual years with the largest wave amplitudes. Contours of spectral power or wave variance are shown in Figs. 6–7, and values are plotted only over regions where the 2-day wave coh^2 is greater than 0.05 (approximately the 50% confidence level) with respect to reference positions at 1 mb, 20°S (January), and 20°N (July). The wave variance sections in Figs. 6–7 are near mirror images of each other, with maxima in the uppermost data levels near 20°S and N, extending in latitude from approximately 10° in the winter hemisphere to 50° in the summer hemisphere. The wave is horizontally in phase over these latitudes, as shown in Fig. 8. The January wave variance structure (Fig. 6) shows a weak secondary maximum near 30°N, which is out of phase horizontally with respect to the main maximum near 20°S (Fig. 8); however, the calculated coh^2 in this region is below significant levels (maximum of 0.12). A similar horizontally out-of-phase region is observed centered near 35°S in July (Fig. 8), but the coh^2 is again very low (0.05). Although these coh^2 values are below formal significance levels, the similar spatial patterns in January and July, together with the observed slow phase variation in these regions, is suggestive of real (albeit weak) atmospheric structure. Note that the corresponding balanced meridional winds would be in phase between hemispheres, as observed by Tsuda et al. (1988). Figure 9 shows the meridional amplitude and phase structure of the 2-day temperature wave from the solstitial normal-mode calculations of Salby (M. Salby 1992, personal communication). This calculated structure is very similar to that observed for January in Fig. 8 (inverted in July), with maximum near 20°S and weak out-of-phase maximum in winter midlatitudes (the calculated winter maximum is 10°–20° poleward of that observed).

The vertical phase structure of the 2-day temperature wave derived from these data is shown in Fig. 10 for both January and July, together with the calculated coh^2 with respect to the 1-mb level. Nearly identical phase structure is found in both months, with an approximate 180° phase shift between 1–2 mb and 10 mb. It should be noted that the vertical resolution of these data is rather coarse (of order 15 km), and that analyses at adjacent pressure levels are not completely independent, so that details of the phase structure in Fig. 10 should be interpreted cautiously. Although the temperature wave variance decreases rapidly below 2 mb in Figs. 6–7, the coh^2 is highly significant between 1 and 10 mb (Fig. 10), and hence the phase reversal between the middle and upper stratosphere is likely a robust result. Also shown in Fig. 10 is the 2-day temperature wave phase structure from the normal-mode calculations of Salby. The calculated structure shows a rapid 180° phase change between 45 and 52 km, qualitatively similar to the observations, but approximately 10 km higher.

4. Summary and discussion

Observations of the 2-day wave in NMC stratospheric analyses has yielded the following characteristics:

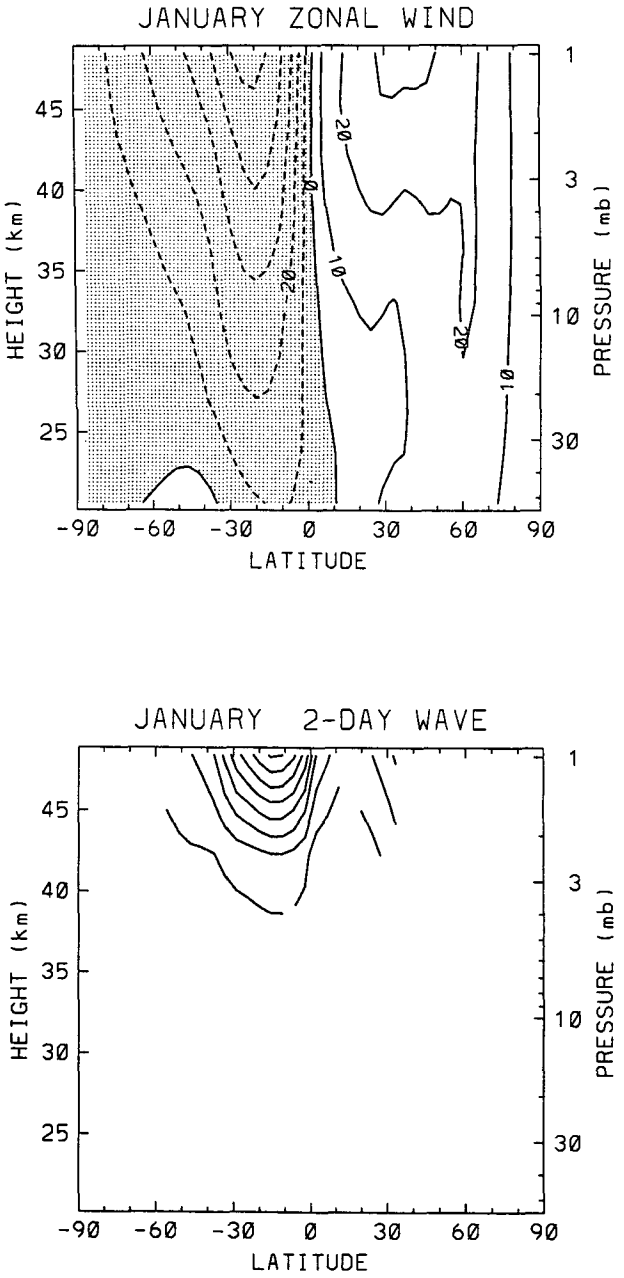

FIG. 6. Bottom panel shows a meridional cross section of 2-day wave temperature variance in January, calculated using data from 1985, 1986, and 1987 (see Fig. 2). Contours are 0.04 K^2, plotted only over regions where the coh^2 is greater than 0.05 with respect to 1 mb, 20°S. The top panel shows the corresponding zonal mean zonal wind.

1) Zonal wavenumber–frequency spectra for traveling temperature waves shows clear maxima for zonal waves 3–4 with periods near 2 days in January (near 20°S) and July–August (near 20°N). The spectra at 20°S are sharply peaked at wave 3, while July has significant contribution for both waves 3 and 4. Individual events are somewhat stronger in January as compared to July.

2) The structure of the 2-day temperature waves is very similar in both January and July. Amplitudes are strongest in the uppermost data levels analyzed here (1–2 mb), centered near 10°–20°S in January and 20°–30°N in July. The latitudinal structure shows in-phase maxima covering approximately 10° in the winter hemisphere to 50° in the summer hemisphere. These

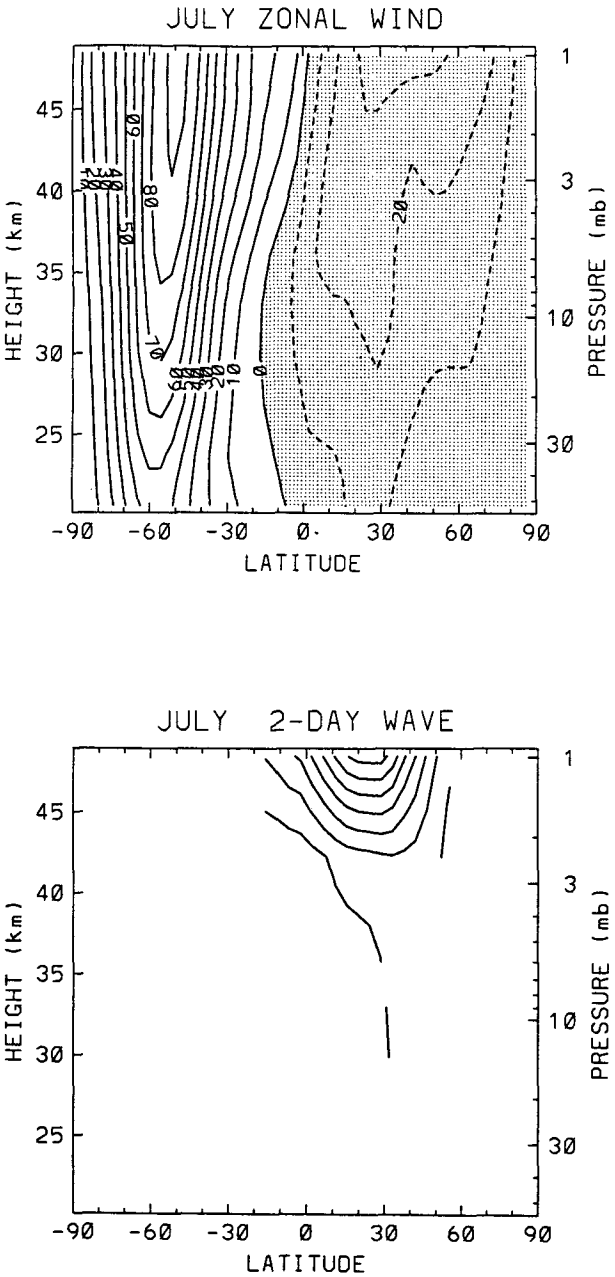

FIG. 7. Meridional cross sections of zonal mean wind and 2-day wave temperature variance, as in Fig. 6, calculated from data covering July 1985, 1986, and 1988 (see Fig. 4).

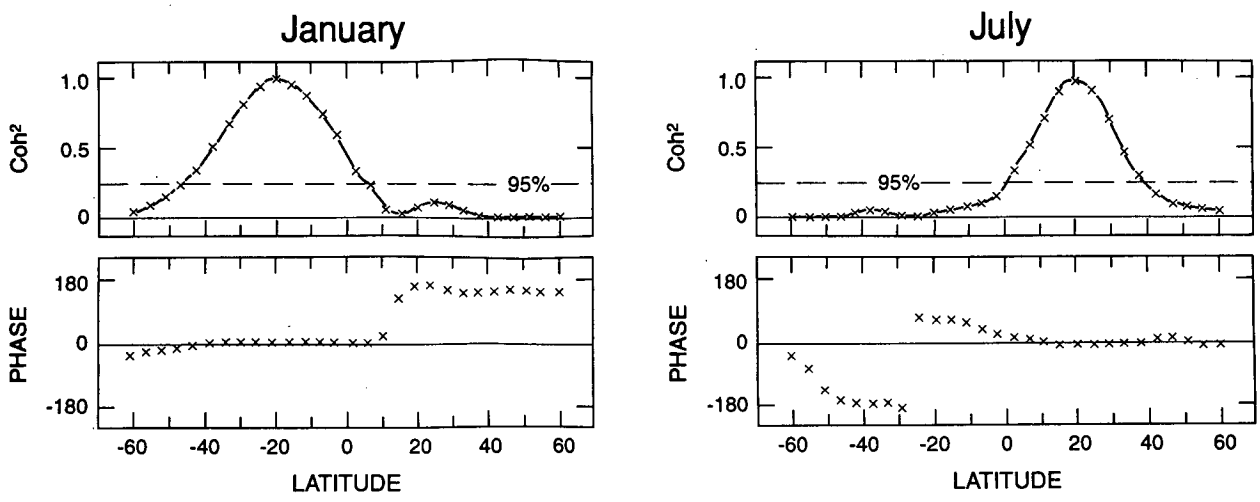

FIG. 8. Latitudinal cross sections of coh^2 and phase for the 2-day wave at 1 mb, for January (left) and July (right), calculated with respect to reference positions at 20°S and 20°N, respectively.

data also show a weak out-of-phase maximum in the winter hemisphere near 30° latitude, but the calculated coh^2 is rather low and thus not definitive. This horizontal out-of-phase behavior in temperature data is similar to the calculated normal-mode structure of Salby (Fig. 9). Note that the temperature structure analyzed here can be misleading in that it suggests that the disturbance is found almost exclusively in the summer hemisphere. The corresponding meridional wind oscillation extends well into the winter hemisphere (e.g., Salby 1981b, his Fig. 8); this accounts for the twice-yearly amplification observed by midlatitude radars (e.g., Muller and Nelson 1978).

Although temperature wave amplitudes are weak at 10 mb, these data show strong statistical coherence between the 1-mb and 10-mb levels. The vertical phase structure is such that these levels are approximately 180° out of phase; the credibility of this observation is enhanced by nearly identical patterns in January and July. The observed rapid vertical phase variation is consistent with the calculation of Salby, although the calculated phase transition region is approximately 10 km higher than observed.

3) Reconstruction of the 2-day wave variance over a five-year data record shows clear evidence for the episodic appearance of the wave in each hemisphere for several weeks following the solstice. These wave episodes occur coincident with or slightly following the strongest zonal mean easterlies at 1 mb.

The most important result here is the observation that generation of the 2-day wave occurs in tandem with or subsequent to periods of negative PV gradients near the

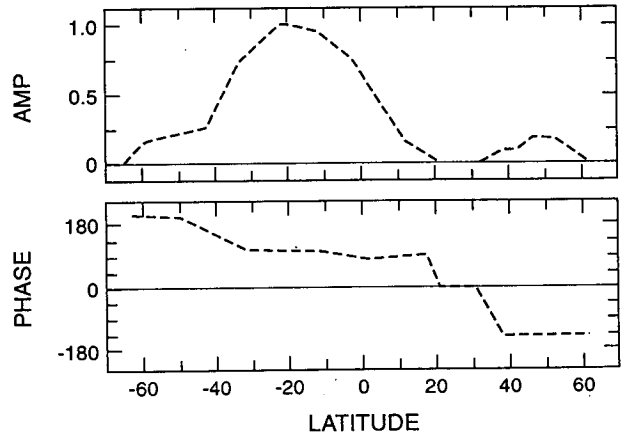

FIG. 9. Latitudinal cross sections of temperature amplitude and phase from the 2-day normal-mode calculation of Salby (1981b). The amplitude has been normalized to a maximum value of 1.0.

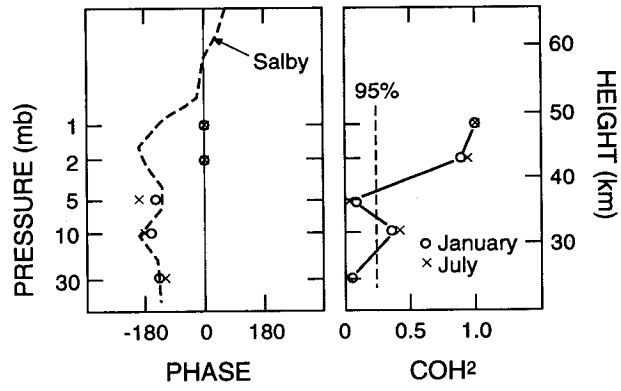

FIG. 10. Left panel shows the vertical phase structure of the 2-day temperature wave, calculated in January (at 20°S) and July (at 20°N). Also shown is the vertical phase structure calculated by Salby (1981b). The right panel shows the analyzed coh^2 for these data with respect to the 1-mb level.

core of the summer easterly jet. Examination of one year in detail shows that wave growth occurs coincident with zonal wind deceleration and removal of the negative PV gradients. These signatures are strong evidence that the 2-day wave grows as a response to instability of the mesospheric easterly jet, as proposed by Plumb (1983) and Pfister (1985).

Overall, the observed meridional and vertical structure of the 2-day wave revealed in these data is in reasonable agreement with the normal-mode calculations of Salby (1981a,b). Coupled with the clear instability signatures shown here, these data suggest that the 2-day wave is some combination of resonant and unstable modes. The near match in wavenumber and frequency of these modes may be one reason why this particular oscillation is so easy to excite and maintain in the real atmosphere.

Acknowledgments. The author thanks Mel Gelman and Jim Miller of NMC for discussions regarding these data. Masato Shiotani provided a review of the manuscript and Murry Salby provided both comments and the calculated wave structures shown in Figs. 9–10. Marilena Stone expertly prepared the manuscript. This work has been supported under NASA Grant W-16215.

REFERENCES

Andrews, D. G., J. R. Holton, and C. B. Leovy, 1987: *Middle Atmosphere Dynamics.* Academic Press, 489 pp.

Burks, D., and C. Leovy, 1986: Planetary waves near the mesospheric easterly jet. *Geophys. Res. Lett.,* **13,** 193–196.

Coy, L., 1979: A possible 2-day oscillation near the tropical stratopause. *J. Atmos. Sci.,* **36,** 1615–1618.

Craig, R. L., and W. G. Elford, 1981: Observations of the quasi 2-day wave near 90 km altitude at Adelaide (35°S). *J. Atmos. Terr. Phys.,* **43,** 1051–1056.

——, R. A. Vincent, G. J. Fraser, and M. J. Smith, 1980: The quasi 2-day wave in the Southern Hemisphere mesosphere. *Nature,* **287,** 319–210.

Gelman, M. E., A. J. Miller, K. W. Johnson, and R. M. Nagatani, 1986: Detection of long-term trends in global stratospheric temperature from NMC analyses derived from NOAA satellite data. *Adv. Space Res.,* **6,** 17–26.

Hayashi, Y., 1971: A generalized method of resolving disturbances into progressive and retrogressive waves by space Fourier and time cross-spectral analysis. *J. Meterol. Soc. Japan,* **49,** 125–128.

Lait, L. R., and J. L. Stanford, 1988: Applications of asynoptic space–time Fourier transform methods to scanning satellite measurements. *J. Atmos. Sci.,* **45,** 3784–3799.

Muller, H. G., and L. Nelson, 1978: A traveling quasi 2-day wave in the meteor region. *J. Atmos. Terr. Phys.,* **40,** 761–766.

Pfister, L., 1985: Baroclinic instability of easterly jets with applications to the summer mesosphere. *J. Atmos. Sci.,* **42,** 313–330.

Plumb, R. A., 1983: Baroclinic instability at the summer mesosphere: A mechanism for the quasi-two-day wave? *J. Atmos. Sci.,* **40,** 262–270.

——, R. A. Vincent, and R. L. Craig, 1987: The quasi-two day wave event of January 1984 and its impact on the mean mesospheric circulation. *J. Atmos. Sci.,* **44,** 3030–3036.

Rodgers, C. D., and A. J. Prata, 1981: Evidence for a traveling two-day wave in the middle atmosphere. *J. Geophys. Res.,* **86,** 9661–9664.

Salby, M. L., 1981a: Rossby normal modes in nonuniform background configurations. Part II: Equinox and solstice conditions. *J. Atmos. Sci.,* **38,** 1827–1840.

——, 1981b: The 2-day wave in the middle atmosphere: Observations and theory. *J. Geophys. Res.,* **86,** 9654–9660.

——, and R. Roper, 1980: Long-period oscillations in the meteor region. *J. Atmos. Sci.,* **37,** 237–244.

Tsuda, T., S. Kato, and R. A. Vincent, 1988: Long period wind oscillations observed by the Kyoto meteor radar and comparison of the quasi-2-day wave with Adelaide HF radar observations. *J. Atmos. Terr. Phys.,* **50,** 225–230.